Journal of Sustainable Development of Energy, Water and Environment Systems

http://www.sdewes.org/jsdewes

Year 2026, Volume 14, Issue 2, 1400669

Original Research Article

Modeling and Simulation of a Variable Irradiance Particle Swarm Optimization Algorithm for Maximum Power Point Tracking in Photovoltaic Systems

Othman M. Hussein Anssari*[*1, 2], Mohammad Ali Badamchizadeh[1], Sehraneh Ghaemi[1]

[1]ITRDC, University of Kufa, Al Najaf, Iraq

[2]Faculty of Electrical and Computer Engineering, University of Tabriz, Tabriz, Iran

e-mail: o.mohammad@tabrizu.ac.ir, mbadamchi@tabrizu.ac.ir, ghaemi@tabrizu.ac.ir, othman.alansari@uokufa.edu.iq

Cite as: Hussein Anssari, O. M., Badamchizadeh, M., Ghaemi, S., Modeling and Simulation of a Variable Irradiance Particle Swarm Optimization Algorithm for Maximum Power Point Tracking in Photovoltaic Systems, J.sustain. dev. energy water environ. syst., 14(2), 1300669, 2026, DOI: https://doi.org/10.13044/j.sdewes.d13.0669

ABSTRACT

The conventional energy sources, like fossil fuels, are considered unsuitable due to pollution; researchers are investigating new ways to source renewable energy, such as solar energy, which is transformed into electrical energy through photovoltaic cells, depending on prevailing weather conditions. The traditional maximum power point tracking techniques face challenges in identifying the maximum power point due to variable weather conditions, thereby diminishing the efficiency of the photovoltaic system. Optimizing the maximum power point tracking process is essential to address this issue, and any effective maximum power point tracking must adapt to changing environmental conditions. This paper presents a simulation and evaluation of a novel variable irradiance particle swarm optimization algorithm to improve the tracking rate and performance under fluctuating weather conditions (unlike the conventional particle swarm optimization methods). This method includes a current-sensing mechanism that detects 5% changes in current to reinitialize the parameters. The contributions of this work are declared in the development of an enhanced particle swarm optimization algorithm fitted for variable irradiance environments, Integration of a dynamic reset mechanism based on real-time current variations, and validation of performance through MATLAB/Simulink simulations using a single PV panel and comparing it with standard maximum power point tracking methods. The performance of the variable irradiance particle swarm optimization algorithm showed improvements in speed with a response time of less than 0.1s, reduced the steady state ripple by 1%, and efficiency for maximum power point tracking of 99%, with statistically validated performance using the Friedman test, confirming its robustness for practical photovoltaic applications.

KEYWORDS

Maximum Power Point Tracking, Photovoltaic system, Particle Swarm Optimization.

*Corresponding author

INTRODUCTION

Solar energy is considered one of the most prominent renewable energy resources in the world since it is abundant and has fewer impacts on the environment than fossil fuels, which are finite and harm the environment [1]. With the growing global demand for energy, Photovoltaic (PV) systems are becoming increasingly popular as a reliable solution [2], [4]. Nonetheless, one of the major issues of concern is the ability to achieve improved efficiency, [5] and this is underscored by the fact that these systems are highly dependent on the prevailing environmental conditions likely to be exhibited through changes in factors like irradiance and temperature [6], [7]. These changes affect the nature of the power-voltage (P-V) characteristics of PV modules [8]. Hence, it becomes challenging for the conventional Maximum Power Point Tracking (MPPT) [9], [10] algorithms to always locate the Maximum Power Point (MPP) (the point at which a solar panel is working at its absolute peak efficiency and generating the maximum possible power. It determined by the PV module's current-voltage characteristics, which depend on environmental conditions, as sunlight and temperature are always changing; this sweet spot is constantly shifting) [11], [13].

Traditional MPPT techniques, such as perturb and observe (P&O) and other algorithms, are often challenged by variable climatic conditions; this results in slow tracking or oscillations around the MPP, leading to losses in system efficiency [14]. These limitations have driven the introduction of advanced soft computing techniques like the Particle Swarm Optimization (PSO) [15], [16]. Many conventional methods for tracking the MPP are less accurate than PSO, a meta-heuristic optic optimization algorithm, as it converges faster [17]. Recently, researchers have learned how to monitor the MPP under different weather conditions using soft computing techniques [18], [19]. Some of them are fuzzy logic control [20], artificial neural networks [21], genetic algorithms [22], and ant colony optimizations [23]. They examine the behavior of their algorithm when there are variations in the solar irradiance of the PV panel. They can track the MPP with minimal fluctuations in power compared with the P&O algorithm. Two previous studies provided significant information on PSO for tracking the maximum power point in PV systems; they present better techniques for MPPT under fixed irradiance conditions. Still, these improved algorithms do not consider the temperature factor, which reveals important limitations [24], [25].

Many studies combined multiple algorithms, [26] and specialized control methods to manage the converter switch and achieve the MPP, such as A study that proposed combining the modified shuffled frog leaping algorithm (MSFLA) with a sliding mode control (SMC) scheme [27], MSFLA with a fuzzy logic controller (FLC) [28], to enhance the efficiency and performance of the designed MPPT for PV systems; the accompanying increased complexity, more parameter setting, and cost constraints are also the issues to be dealt with. A study that presents a way of improving the performance of MPPT controllers in PV systems via the integration of PSO and SMC [29]. Nevertheless, the algorithmic enhancement presented in this paper, as well as the use of multiple algorithms in general, is of value for future studies and applications [30]; however, the obstacles related to the complexity, hard implementation, and functionality, such as chattering, as well as the computational burden, all pose some interesting problems that deserve to be studied [31]. Another study focuses on the major strides achieved in using the mine blast optimization algorithm (MBOA) in the MPPT of solar PV systems. The MBOA-MPPT technique has shown greater potential for increasing energy extraction efficiency. Whereas the MBOA-MPPT technique is a major improvement in the method used to harvest solar energy, multiple algorithms pose some challenges that need a close look [32]. To that end, future studies can help provide the foundations for advanced and improved MPPT algorithms that are less prone to inaccuracies as well as are more efficient in fulfilling the continually rising

power requirements of new grid-connected SPV systems; these are some of the effects that should be taken into account in further experimental and theoretical studies of MPPT control schemes for practical implementations [33].

This paper introduces an improved Variable Irradiance Particle Swarm Optimization (VIPSO) algorithm for better partisan MPPT performance under varying climatic conditions. The basic idea behind this algorithm is that solar irradiance is unpredictable, and the algorithm modified to adjust when irradiance changes by 5% to help the algorithm re-explore the search space. This threshold was determined based on the system's dynamic response to environmental changes. Minor fluctuations below 5% have an insignificant effect on the PV power–voltage characteristic curve and handled by the standard iterative update process of the algorithm. However, a larger irradiance variation alters the curve substantially, rendering the previously optimized duty cycle less effective. Therefore, reinitializing the particles when the irradiance change surpasses 5% enables the algorithm to rapidly adapt to new operating conditions while avoiding unnecessary computational effort caused by frequent reinitializations. This initialization resets the particles' positions, velocities, and best solution in response to major irradiance changes to adapt the system's operation; as a result, it ensures near-optimal power output even under dynamic environmental conditions.

The improved VIPSO applied to PV systems, optimizing the converter duty cycle based on the solar panel's power output. In this case, the algorithm adjusts the duty cycle to track the MPP, with power output as the objective function. When irradiance changes significantly, the modified PSO resets key parameters, such as best positions and velocities, to ensure continued MPPT. Without this adjustment, the algorithm may struggle to follow the MPP after large fluctuations in irradiance, as previous best solutions become irrelevant. The effectiveness of the improved algorithm validated through MATLAB/Simulink simulations, and its performance compared with conventional MPPT techniques. The results show significant improvements in tracking speed, accuracy, and overall system efficiency, offering a robust solution to maximize the power output of PV systems. The proposed system includes a single PV panel, DC-DC converter, MPPT technology controller, and load, as shown in Figure 1. The PV panel has sensed voltage and current given to the controller (VIPSO) to control the converter's duty cycle while in MPP operation.

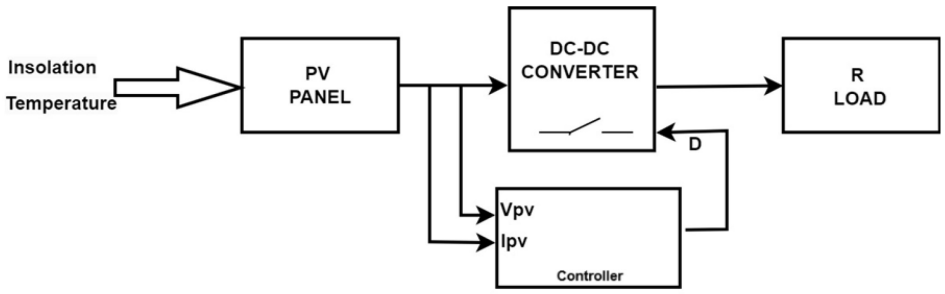

Figure 1. Block diagram of the PV system

Main Properties of the Utilized Photovoltaic Modules

The solar power system was a Soltech 1STH-250-WH solar cell simulating the solar cell behavior by means of a diode model. Solar radiation and temperature variations were applied on the system after a certain period, and the MPPT process was governed by an adaptive SMC (ASMC) algorithm, which was augmented with the application of PSO.

The single-diode PV cell model illustrated in the following mathematical form, shown in Figure 2: PV panel model [34]. The model composition includes an equivalent series and parallel

resistance, a current source, and a single diode [3]. Irradiation is the main factor, together with the temperature change, affecting the power output of a solar panel. The current varies directly with the irradiance change in the same direction; contrariwise, the voltage varies in inverse ratio to the temperature. The power output of the solar panel at any point is given by [29], [34], [35]:

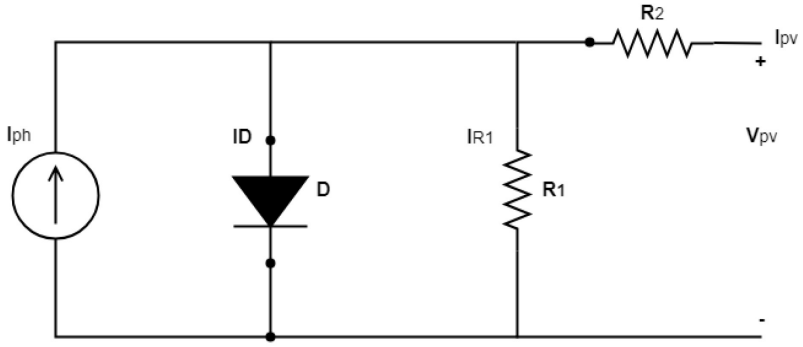

Figure 2. PV panel model [34]

$$P = V \times I \tag{1}$$

Where: P, is the power measured in W, V, is the voltage in V, and I, is the current in Amp. The characteristic equation can be expressed mathematically by using the Kirchhoff law with the following formulas [29]:

$$Ipv = Iph - Id - IR1 \tag{2}$$

Where: Iph, is the photocurrent generated by the solar radiation, Id is the diode current, and $IR1$, is the shunt current. The diode current is equal to:

$$Id = Is * \left(\exp\left(\frac{qVpv}{nkt}\right) - 1\right) \tag{3}$$

Where: Is, is the reverse saturation current of the diode; q, is the electron charge; k, is the Boltzmann's constant; t, is the temperature in Kelvin; and n, is the ideality factor.
Shunt current is equal to:

$$IR1 = Vpv + (R2\frac{Ipv}{R1}) \tag{4}$$

Then, solving equation (2) by substituting equations (3) and (4).

$$Ipv = Iph - Is * \left(\exp\left(\frac{qVpv}{nkt}\right) - 1\right) - Vpv + (R2\frac{Ipv}{R1}) \tag{5}$$

The MPP is that point where voltage and current multiplied together are at their maximum. The power at MPP approximated by this equation:

$$P_{max} = V_{mp} \times I_{mp} \quad (6)$$

Where V_{mp}, and I_{mp} are the voltage and current at the MPP. A typical solar panel has a power rating of 250.205 W; this is the maximum power that the panel can produce under standard test conditions. The panel has two inputs: input 1 is the sun irradiation, in W/m^2, and input 2 is the cell temperature, in Celsius. (The ambient condition defined as irradiance of 1000 W/m^2 and a temperature of 25°C.). Open − circuit voltage (V_{oc}) the maximum voltage that the panel can produce in no load condition (for a condition when current is not being drawn from the panel) is equal to 37.3 V and the Short-circuit current (I_{sc}) of 8.66 A, which is the maximum current the panel can deliver when the load resistor equals zero ohms (when the output terminals touch each other) and is used in this work and most of the solar power systems. To introduce general facts about the main characteristics and equations, and depict a simplified diagram. In addition to the IV point representing the maximum power capacity, which seen to give an overall power. **Table 1**: Specifications (datasheet) of the PV panel presents the specification of the single PV module that used in the proposed model.

Table 1. Specifications (datasheet) of the PV panel

Maximum power ($Pmax$)	**250.205 W**
The voltage at Pmax (Vmp)	30.7 V
Current at Pmax (Imp)	8.15 A
Short-circuit current (Isc)	8.66 A
Open-circuit voltage (Voc)	37.3 V
Temperature coefficient of Isc	0.086998 %/°C
Temperature coefficient of Voc	-0.36901 %/°C

The $I-V$ and $P-V$ characteristics curves help visualize how a PV module assists in visualizing the performance of the PV module, as shown in **Figure 3**: IV, and PV characteristic of the PV panel. An explanation of the curves as in below:

$I-V$ Curve: Starts at the I_{sc} at no voltage across the PV cell. As voltage rises, the current stays nearly flat and drops rapidly once it reaches the vicinity of the V_{oc}.

$P-V$ Curve: At zero, power starts when the voltage of the rise is zero. Power rises and attains its maximum value, the MPP, and then declines to zero as voltage draws closer to the V_{oc}. The irradiance, while the voltage is inversely proportional to the temperature. After V_{oc}, it flattens and then bends again, the implication being that current reduces with an increase in voltage.

Pmax: The point at which the amount of electrical power that produced in the circuit reaches the highest level. These diagrams provide excellent visualization of voltage and current behavior and show that power at that point is at its maximum.

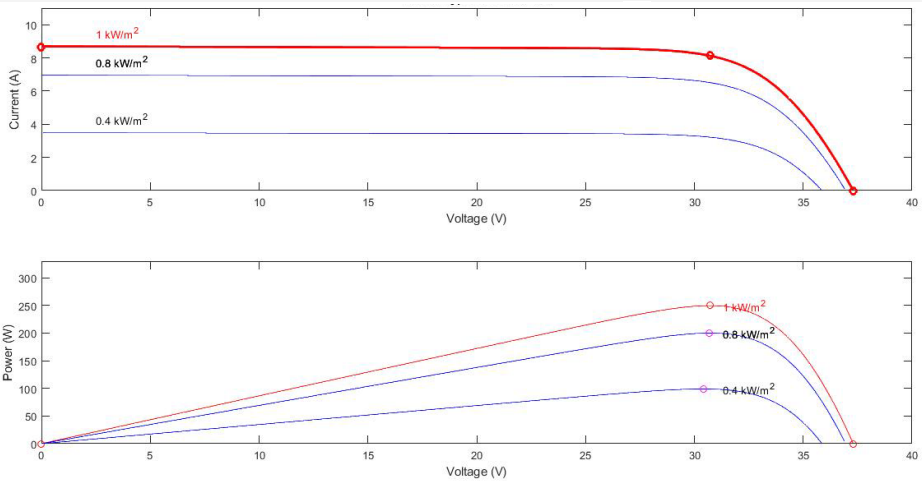

Figure 3. IV, and PV characteristic of the PV panel

As the temperature rises, the Voc decreases, and thus power output reduces as well. At the same time, while the current density decreases, Isc increases with temperature. For the current, they are in proportion with irradiance. At the same time, the voltage varies slightly as irradiance increases, and commonly utilized in residential or small commercial scale PV systems. With such methods as MPPT, the system can identify when it is below optimal efficiency, which tied to the tracking of MPP.

Boost Converter

A DC-DC boost converter converts the low-voltage input to a higher-voltage output. The converter works like a normal boost converter, with energy storage and a low-pass filter incorporated into it. The components of the boost converter, as shown in **Figure 4**: Boost Converter Circuit Diagram **[36]**, are from an inductor (l), which charges when the switch (transistor) is ON and discharges whenever the switch is OFF. A capacitor to convert, store, and smooth energy and provide for a low output voltage fluctuation. It could be placed in the vicinity of the input for stabilization and/or coupled to the first ends of at least two bars for stiffness, typically filtering the output **[36]**. An energy control transistor, for instance, is the MOSFET switch that switches the energy flow between the inductor and the capacitor. Moreover, a diode facilitates an individual current flow, which means that energy can freely flow to the load, but reverse current prevented when the switch is on. In addition, a resistive load stands for a load that draws the output power.

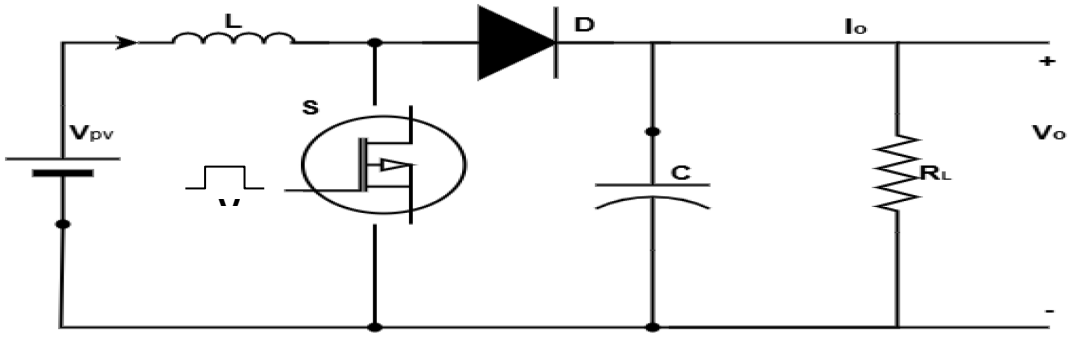

Figure 4. Boost Converter Circuit Diagram **[36]**

The Boost Converter Works in Two Modes During Each Switching Cycle (Working Principle):

Mode 1 when Switch is ON: The switch is in the closed position, and current is now circulating on the in and out of the inductor. During this phase, the inductor stores energy in its magnetic field and the diode is reverse-biased, so no current flows through it to the output.

Mode 2 when the switch is OFF: the switch is open, and the energy that was stored in the previous inductor is discharged. This makes the inductor act as a current source and dump energy through the diode, producing the output current. This is the second phase, where the voltage across the input added to that across the inductor, leading to a large output voltage. The boost converter follows the principle of energy conservation, and the output voltage (V_{out}) can be expressed as a function of the input voltage (V_{in}) and the duty cycle (D), which is the ratio of the on-time of the switch to the total period. as shown below [37]:

$$V_{out} = V_{in}/(1 - \mathrm{D}) \tag{7}$$

Equation 7 shows that the output voltage is higher than the input voltage for a duty cycle greater than zero. The voltage across the inductor (V_l) expressed as shown below:

$$V_l = V_{pv} - V_o \tag{8}$$

The inductor current increases linearly during the switch's ON phase and decreases during the OFF phase. The current ripple in the inductor (ΔI_l) can be expressed as a function of (V_{in}), (D), ($_l$), and the switching period (T), which is the inverse of switching frequency (f_s). As shown below:

$$\Delta I_l = V_{in} \cdot D \cdot T/_l \tag{9}$$

The capacitor reduces voltage ripple at the output ($\Delta Vout$) can be expressed as a function of output current (I_{out}), switching frequency (f_s), and the output capacitor value (C_2). As shown below:

$$\Delta V_{out} = I_{out} * D/(f_s * C_2) \tag{10}$$

In a boost converter circuit diagram, a configuration with two capacitors, C_1 represents the input-side capacitor (which helps stabilize input voltage by reducing any voltage ripples or fluctuations from the input source, providing a smoother input to the boost converter). It might be placed across the input for filtering. At the same time, C_2 is the other capacitor on the output side to ensure that the output voltage is smooth and free of ripples, delivering a more stable DC voltage to the load (filters output voltage). The values of C_1 and C_2 are chosen based on the desired voltage ripple and the power level of the converter. Larger capacitors reduce voltage ripple but can slow down the system's response time.

Moreover, the value of the inductor affects current ripple and efficiency, as a larger inductor assists in reducing the current ripple but will also add more to its size and, therefore, increase its cost. Apart from the limitations of the duty cycle, since the duty cycle is very close to one, the output voltage rises; however, the efficiency is low due to losses in the switch and diode. This configuration can be part of any application that demands conversion efficiency with a specific requirement for voltage boosting, that is, in PV applications [38]. The parameters for the DC-DC converter that are used in this paper are 30 e-4 H for the inductor, 100 e-6 F for the capacitor, 50 Ω for the resistive load, and 10 kHz for the switching frequency.

Maximum Power Point Tracking using Particle Swarm Optimization

The generalization of the PSO algorithm qualifies this work as advancing the MPPT for PV systems under different weather conditions. It also provides a solution to most of the prevailing MPPT approaches known for their inefficiency in tracking the MPP suitably [39], [40]. The ability to promote better performance and guaranteed reliability of PV power stations makes it a promising solution. When the demand for renewable energy becomes even bigger, the necessity of such intelligent algorithms will play an important role in increasing energy production and creating better solutions [41].

The basic idea behind PSO is to simulate the behavior of a swarm of particles moving through a search space, where each particle represents a potential solution to the optimization problem. The particles move through the search space based on their position and velocity and the best position any particle in the swarm finds. This allows PSOs to explore various potential solutions, and converge on an optimal solution over time. The mean squared error (MSE) between the boost converter's actual and expected output guides the optimization. It optimizes the SMC control parameters; once optimal SMC gains found, they used to adjust the step size in P&O algorithms for MPPT.

Improved Variable Irradiance Particle Swarm Optimization

The improved VIPSO algorithm optimizes an MPPT system in light irradiance. It is modified to work in a dynamic environment, which is not the case with a simple PSO, and is a universal algorithm suited for static optimization problems. The improved VIPSO has many merits over the simple PSO, as shown in **Table 2**: The Summary of Differences between the Improved VIPSO and the Simple PSO Algorithm contrasts with simple PSO, which does not include real-time MPPT and hence does not require such tuning as the improved VIPSO. The merits of the improved algorithm have been confirmed by simulations performed with MATLAB/Simulink. These simulations made for various conditions, showing the algorithm's efficiency in real-life situations. The experimental outcome demonstrated that the new algorithm is faster and more effective than several other methods existing in the literature.

Table 2. The Summary of Differences between the Improved VIPSO and the Simple PSO Algorithm

Feature	Improved VIPSO	Simple PSO
Adaptation to Irradiance	Resets on significant irradiance change	No adaptation to changing inputs
Objective Function	Real-time control of duty cycle for MPPT	General static optimization

Feature	Improved VIPSO	Simple PSO
Reinitialization	Yes, when conditions change.	No reinitialization mechanism
Real-Time Response	Designed for real-time duty cycle control	No real-time control constraints
Handling Ripple/Overshoot	Attempts to minimize ripple/overshoot	Not applicable to simple PSO
Velocity Update	Updates duty cycle based on PV system	General update for abstract positions

Key Mathematical Equations of the Improved Variable Irradiance Particle Swarm Optimization

The modified algorithm VIPSO uses mathematical equations to update duty cycles (particle velocities and positions), evaluate energy, and determine the best solution. The main mathematical expressions derived from the improved algorithm implementation are as follows:

1. Power calculations:
   - For the voltage given and current, the power is calculated as:

$$P = V_{pv} * I_{pv} \tag{11}$$

   - Where: V_{pv}, and I_{pv} are the panel voltage and current.
2. Particle movement (velocity update):
   The velocity update for each particle i is influenced by its personal best position p_{besti}, its current position d_{ci} (duty cycle), and its global best position g_{besti}. The updated velocity v_i is given by:

$$v_i = w * v_i + C_1 * r_1 * (p_{besti} - d_{ci}) + C_2 * r_1 * (g_{besti} - d_{ci}) \tag{12}$$

Where: w is the inertia weight (controls the influence of the previous velocity), $c1$ is the cognitive coefficient (pull toward the particle's own best position), $c2$ is the social coefficient (pull toward the global best position), r_1 and r_2 are random numbers between 0 and 1, p_{besti} is the best duty cycle found by particle i, d_{ci} is the current duty cycle of particle i, $g_{besti}$is the best global duty cycle found among all particles.

3. Duty Cycle Update: Depending on the particle's new velocity vi its new duty cycle dci is updated:

$$d_{ci} = d_{ci} + v_i \tag{13}$$

Where the duty cycle is constrained within [0, 1]:

$$d_{ci} = \begin{cases} 1 & if\ d_{ci} > 1 \\ 0 & if\ d_{ci} < 0 \\ d_{ci} & otherwise \end{cases} \quad (14)$$

4. Global Best Selection: By finding the particle with the highest energy (after evaluating the performance of all particles (energy output)), the global best g_{best} is updated.

$$g_{best} = \max\ (p_{best}) \quad (15)$$

Where: p_{best} is the vector of best power values for all particles.

5. Condition for reinitialization (Irradiance Change): The algorithm re-initializes the particle positions and velocities if the change in radiation is large (greater than 5%). The condition for re-initialization is:

$$\frac{|Irradiance - p_{prev}|}{p_{prev}} \geq 0.05 \quad (16)$$

Where: $Irradiance$ is the current irradiance, and p_{prev} is the previous power.

6. Closeness Check: The algorithm ensures that the absolute difference between the cycles of any two particles is less than 0.1, as it checks whether the cycles of all particles are "close" to each other:

$$closness = (|d_{ci} - d_{ci}| < 0.1 \quad \forall i, j) \quad (17)$$

7. Iteration Limit Reset: the algorithm will reset when the number of iterations exceeds a threshold.

The Pseudocode of the Proposed Algorithm Explained in the Steps Below:

1. Start

- Begin the process.

2. Initialize parameters

- Set up initial parameters:
  - u = 0
  - $d_{current}$ = 0.5 (initial duty cycle)
  - g_{best} = 0.5 (initial global best duty cycle)
  - dc = randomized duty cycles between 0.1 and 0.9 for all particles.
  - Arrays p, v, and p_{best} are initialized as zeros.
  - Boolean $closeness$ = false.

3. Calculate Power (P)

$P = V_{pv} * I_{pv}$

4. Evaluate Power for Current Particle (u)

- If u >= 1 and u <= $n\_particle$:
  - Calculate $current\_power = V_{pv} * I_{pv}$
  - Compare $current\_power$ to p(u):
    - If $current\_power$ is greater, update $p(u)$ and set $p_{best}(u)$ to .

5. Update Particle Index (u)

- Increment u by 1.
- If $u > n\_particle + 1$, reset $u = 1$.

6. Global Best Update

- If $u == n\_particle + 1$:
  - Find the particle with the maximum power, $g_{best} = p_{best}(idx)$.
  - Update the velocity v and duty cycle dc for each particle using the helper functions $updatevelocity$ and $updateduty$.

7. Duty Cycle Update

- Update the current duty cycle ($d_{current}$) using the best duty cycle of the particle with the maximum power ($dc(idx)$).

8. Irradiance Check

- If the irradiance has changed significantly ($|Irradiance - P_{prev}| / P_{prev} >= 0.05$):
  - Reinitialize the parameters (idx, $d_{current}$, g_{best}, p, v, P_{best}, dc) as in step 2.

9. Closeness Check

- If all duty cycle differences are smaller than 0.1 ($closeness = true$):
  - Set $bool = 1$.

10. Iteration Limit Check

- If the algorithm exceeds 70 iterations without improvement ($k > 70$):
  - Reinitialize all parameters as in step 2.

11. Output Results

- Output the calculated power P and the best duty cycle D.

12. End

- End the process.

Proposed Model and the Simulation Results

This paper aims to maximize the energy output of the PV system during changing environmental conditions (changes in solar radiation and temperature). **Figure 5**: Proposed model circuit diagram provides a more detailed explanation of the idea presented for optimization using an improved VIPSO algorithm for PV systems. The basic idea behind the VIPSO algorithm is that it modified to adapt to dynamic solar irradiance conditions. When irradiance changes by more than 5%, the algorithm resets particle positions, velocities, both the P_{best} and g_{best}, and the best solutions to rediscover the search space. This reinitialization helps the algorithm adjust the operating conditions of the solar panel in response to fluctuating irradiance levels. It manipulates the converter's duty cycle based on the solar panel's power output. In the VIPSO model, particles represent candidate duty cycles, and the algorithm fine-tunes these values to reach the MPP. The solar panel's power output serves as the objective function to optimized, ensuring real-time tracking of MPP. A 5% irradiance change chosen as the reset threshold to distinguish minor fluctuations, which do not significantly affect the MPP, from larger variations that alter the PV characteristics and require reinitialization of the swarm for faster convergence. This value was determined empirically through simulation, where smaller thresholds led to excessive reinitializations, and larger ones caused slower adaptation to changing conditions.

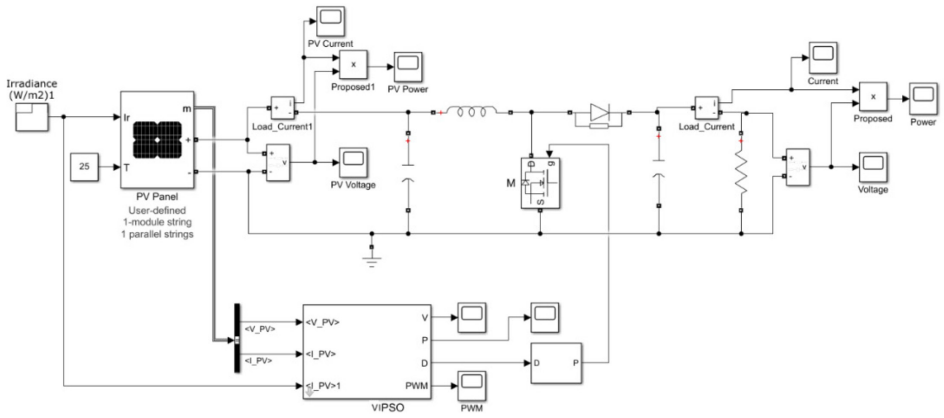

In the enhanced version of VIPSO, velocity updates are constrained to ensure the calculated duty cycle remains within the valid range (between 0 and 1) for the PV system's DC-DC converter. In addition to the standard components of inertia (w), cognitive (C_1), and social (C_2) factors, the algorithm ensures the velocity is applied correctly to adjust the duty cycle. The parameters of the modified VIPSO tuned for real-world electrical systems, where overshoots and ripples can threaten stability. By adjusting the duty cycle and resetting particles when convergence stalls, the algorithm minimizes oscillations and smoothly leads the system to MPP, reducing the risk of instability. The parameters of the VIPSO algorithm configured to ensure fast convergence and stable tracking performance. The population initialized with 20 particles, and the problem's dimensionality was set to 50, representing the number of parameters to optimize. The cognitive and social acceleration coefficients were both assigned a value of 2, providing a balanced influence between individual and global best position during the optimization process.

The purpose of connecting the solar panel to the DC-DC boost converter is to allow the power to deliver and the voltage levels to changed, as a DC-DC converter used to produce the largest amount of power from the solar panel and match the output of the PV panel with the load. The

system's performance improved by transferring energy efficiently through the converter's performance. The circuit starts with the implementation of a 250.205 W solar cell array with two inputs: input 1 represents the solar radiation that varies within these specific times [0, 1, 2, 3] seconds, and with these variable capacities [0.4, 0.8, 1, 0.8] * 1000 W/m^2 irradiance hypothetically as shown in **Figure 6**: Solar irradiance with time, and input 2, represents the constant temperature of 25°C. The conducted tests (unrealistic hypothesis tests) aim to determine the accuracy and reliability of the proposed algorithm through a series of comprehensive assessments. These assessments will evaluate its ability to track the MPP across various weather conditions.

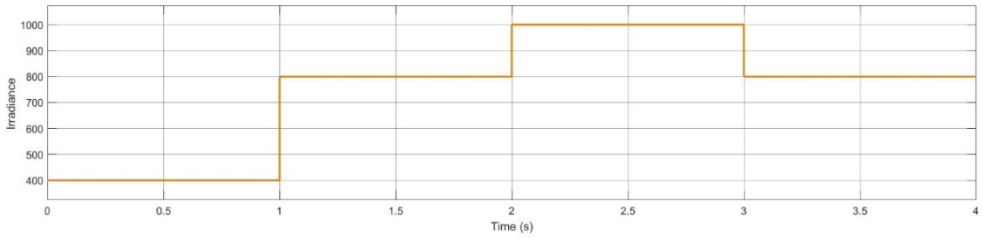

Figure 6. Solar irradiance with time

The following figures present detailed simulation results of the PV system under varying weather conditions. **Figure 7**: Module output a) voltage, b) current, and c) power highlights the performance of the VIPSO algorithm when the solar panel experiences fluctuating irradiance levels, as depicted in Figure 6. Consequently, **Figure 7** (a), (b), and (c) sequentially illustrate the voltage, current, and power output of the proposed algorithm, accounting for changes in irradiance.

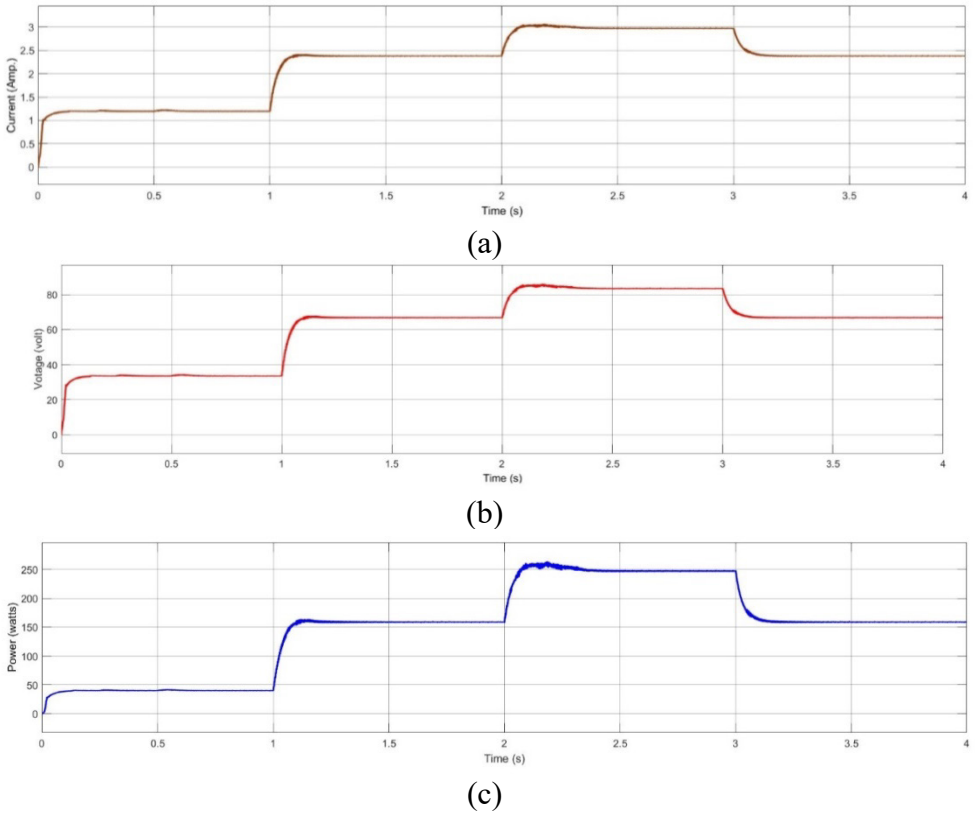

Figure 7. Module output a) voltage, b) current, and c) power

Figure 8: Response time and overshoot provides a more comprehensive analysis by evaluating the effects of different amounts of insolation by zoomed in enough to see the detailed response. These fluctuations encompass cases of solar radiation increasing by a magnitude of 400 W/m², as specifically indicated at time zero, up to 800 W/m², at the first second, up again to 1000 W/m², at the second two, and down to 800 W/m², at the third second. The analysis conducted reveals a minimal impact on the observed overshoot in the proposed method presented, amounting range of (zero watts at 0.1s and 3.1s as shown in **Figure 8**: Response time and overshoot (a), and (d) sequentially, 2 watts at 1.1s as shown in **Figure 8**: Response time and overshoot (b), and about 10 watts at the 2.08s as shown in **Figure 8**: Response time and overshoot (c). On the other hand, the improved algorithm demonstrates a significant improvement in response time, especially when the weather changes frequently, with recorded values ranging from 0.1s, as shown in **Figure 8**: Response time and overshoot (a), (b), (c), and (d).

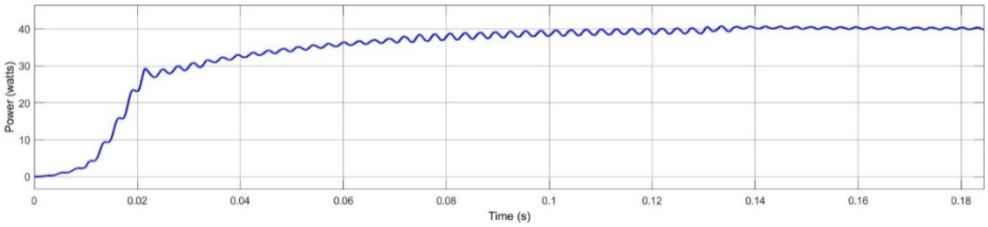

(a)

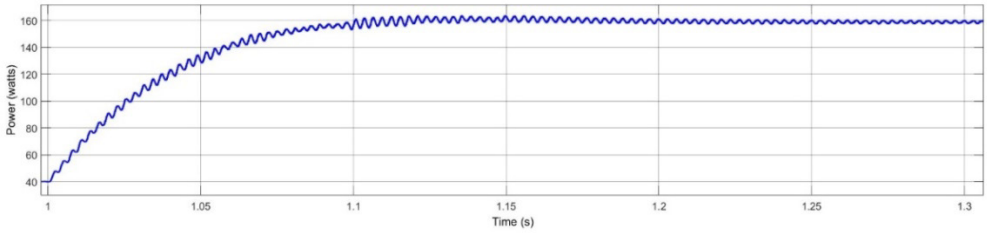

(b)

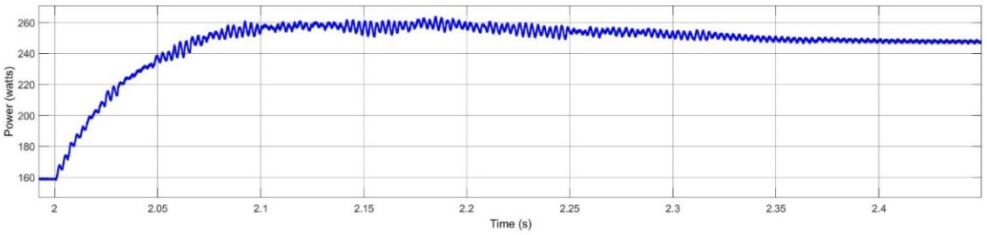

(c)

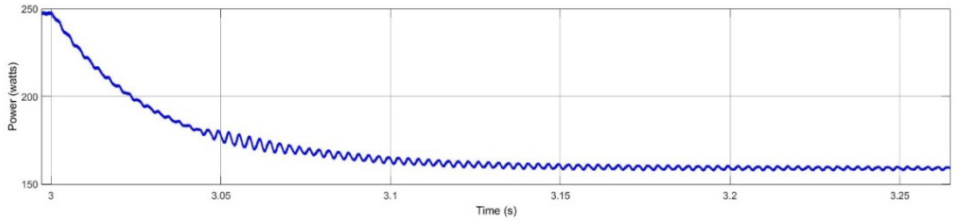

(d)

Figure 8. Response time and overshoot

The improved algorithm shows stable performance, with negligible fluctuations around the MPP at most points with the weather change, with values ranging about 1%, which is the minimum ripple measured at time 1.9 s, as shown in **Figure 9**: Output power fluctuation, showing performance stability at different time intervals: (a) 0.95 s, (b) 1.9 s, (c) 2.9 s, and (d) 3.9 s. (b), 2.9 s, as shown in **Figure 9**: Output power fluctuation, showing performance stability at different time intervals: (a) 0.95 s, (b) 1.9 s, (c) 2.9 s, and (d) 3.9 s. (c), and 3.9 s, as shown in **Figure 9**: Output power fluctuation, showing performance stability at different time intervals: (a) 0.95 s, (b) 1.9 s, (c) 2.9 s, and (d) 3.9 s. (d); moreover, the maximum ripple 1.7% is measured at time 0.95 s, as shown in **Figure 9**: Output power fluctuation, showing performance stability at different time intervals: (a) 0.95 s, (b) 1.9 s, (c) 2.9 s, and (d) 3.9 s. (a) sequentially, as it calculated:

$$Power\ Ripple\ (\%) = \frac{Pmax - Pmin}{Pavg} \times 100 \tag{18}$$

Moreover, Efficiency is calculated as $(average\ power\ /\ maximum\ power) * 100\%$. This equation provides the average MPPT formula for determining efficiency. **[42]**:

$$\eta_{MPPT\ (Avg)} = \frac{\int P_{MPP\ (t)} dt}{\int P_{MPP\ (t)} * dt} \times 100 \tag{19}$$

$P_{MPP(t)*}$, which is the theoretical maximum power that can be reached, is calculated using the PV model. $P_{MPP(t)}$ is the actual power that the MPPT algorithm can produce. **Figure 9**: Output power fluctuation, showing performance stability at different time intervals: (a) 0.95 s, (b) 1.9 s, (c) 2.9 s, and (d) 3.9 s. (c) at 2.9's efficiency equals (247.5/250) * 100, or 99%.

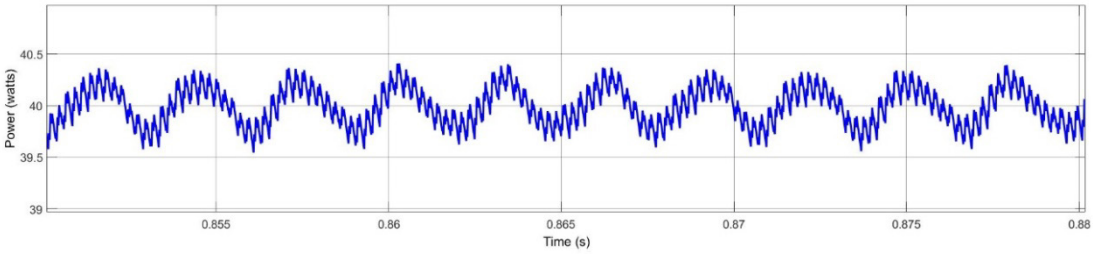

(a)

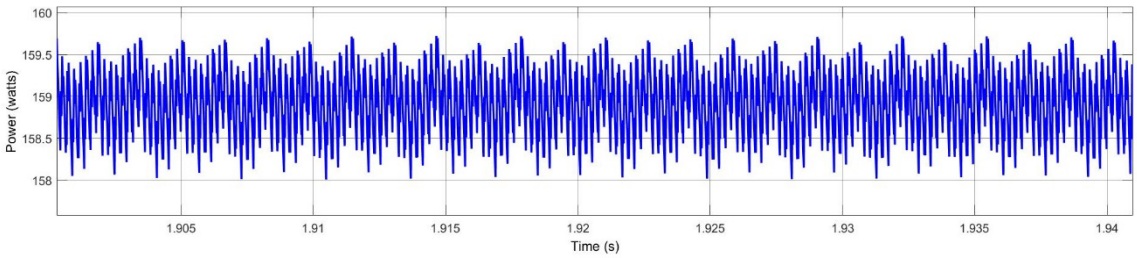

(b)

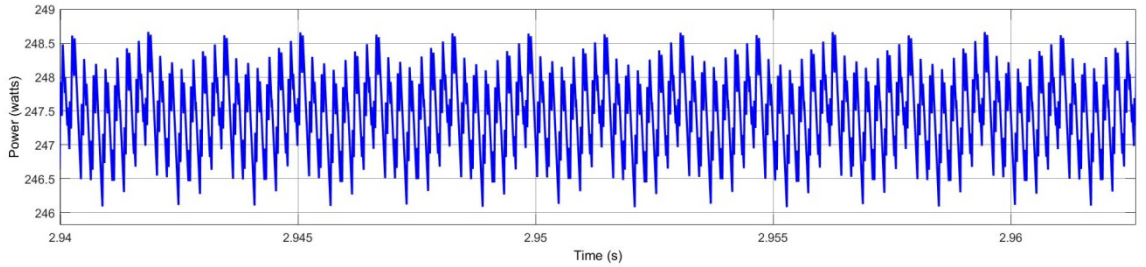

(c)

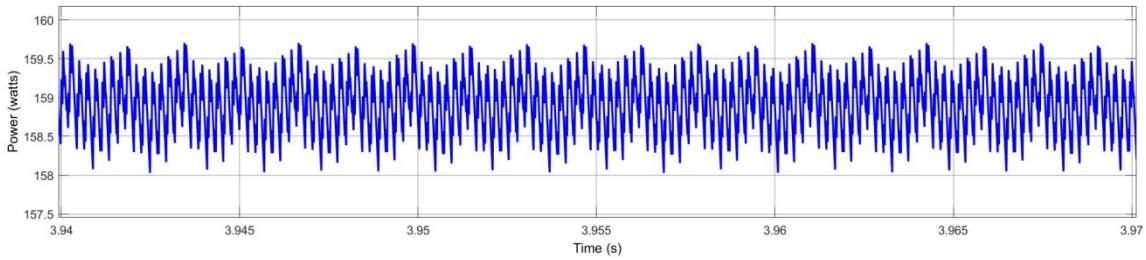

(d)

Figure 9. Output power fluctuation, showing performance stability at different time intervals: (a) 0.95 s, (b) 1.9 s, (c) 2.9 s, and (d) 3.9 s.

Table 3. Results summary for the algorithms that used in previous studies provides a comprehensive evaluation by comparing the results of previous studies that employed various algorithms used for solar irradiance variations comparable to those adopted in this work, ensuring that the performance comparison is fair and scientifically meaningful. Each algorithm's results summarized, including key metrics such as efficiency, response time, overshoot, and ripple. These results enable a direct comparison between the proposed improved VIPSO algorithm and the outcomes from earlier research. The **Table 3**: Results summary for the algorithms that used in previous studiesdemonstrates that the proposed algorithm excels in fast-tracking capability, stability, and tracking efficiency.

Table 3. Results summary for the algorithms that used in previous studies

Reference Number	Algorithm	Efficiency %	Response time (s)	Overshoot (W) %	Ripple (W) %
[43]	Krill herd	99	0.17	---	5
[44]	Improved P&O	95	---	---	---
[45]	SMPI	---	0.009	---	---
[45]	Second-order proportional-integral (2P2Z)	---	0.018	6.4	---
[45]	SMC	---	0.008	3.2	---
[46]	DISMC	99	---	---	---

Reference Number	Algorithm	Efficiency %	Response time (s)	Overshoot (W) %	Ripple (W) %
[47]	FSSO	99	---	---	---
[27]	MSFLA-SMC	99	---	---	---
[31]	PSO-SMC	---	0.052	3	0.019
[31]	Conventional P&O	---	0.234	11.7	0.17
[48]	SMC-PSO	96.4	---	---	---
[32]	Mine blast optimization algorithm (MBOA)	99.5	0. 065	---	---
[49]	Quantum neural network controller	99	---	---	---
[50]	Improved adaptable step-size P&O	99	0.003	---	9.98
[28]	MSFLA-fuzzy logic controller (FLC)	99	0.13	---	---
Proposed	VIPSO	99	0.10 avg	<1%	1.7%

The VIPSO algorithm demonstrates excellent performance in terms of output power ripple, maintaining fluctuations around the MPP below 1.7% even under rapidly varying irradiance and constant temperature conditions. This low ripple represents the main strength of the proposed method, ensuring stable power delivery and minimal oscillations around the operating point. However, the response time of VIPSO is slightly higher compared with some of the other methods considered, due to the iterative convergence process and the reinitialization mechanism triggered by significant irradiance changes. This trade-off between ripple reduction and response speed reflects the algorithm's prioritization of stability and energy yield over extremely fast tracking. For practical PV system implementations, this low ripple can be particularly advantageous, as it reduces stress on power electronic converters and downstream loads, whereas the modest increase in response time remains within acceptable limits for most dynamic solar scenarios.

Tests for Robustness

The tests conducted aim to ascertain the accuracy and dependability of the proposed algorithm through a thorough assessment (which are unrealistic hypothesis tests). These assessments will examine its capability for tracking the MPP under various weather conditions, which may present significant challenges for such an algorithm. Robustness tests in **Figure 10**: The occurrence of random fluctuations in amounts of incoming solar irradiance while concurrently

maintaining a constant temperature of 25 *Co*, evaluates algorithm performance through substantial stress-testing scenarios using a single PV module in simulation. Which included the fact that there are unplanned variations in irradiance while maintaining a constant temperature level of 25°C, as illustrated in **Table 4**. The table also reports the resulting performance metrics obtained under these varying conditions.

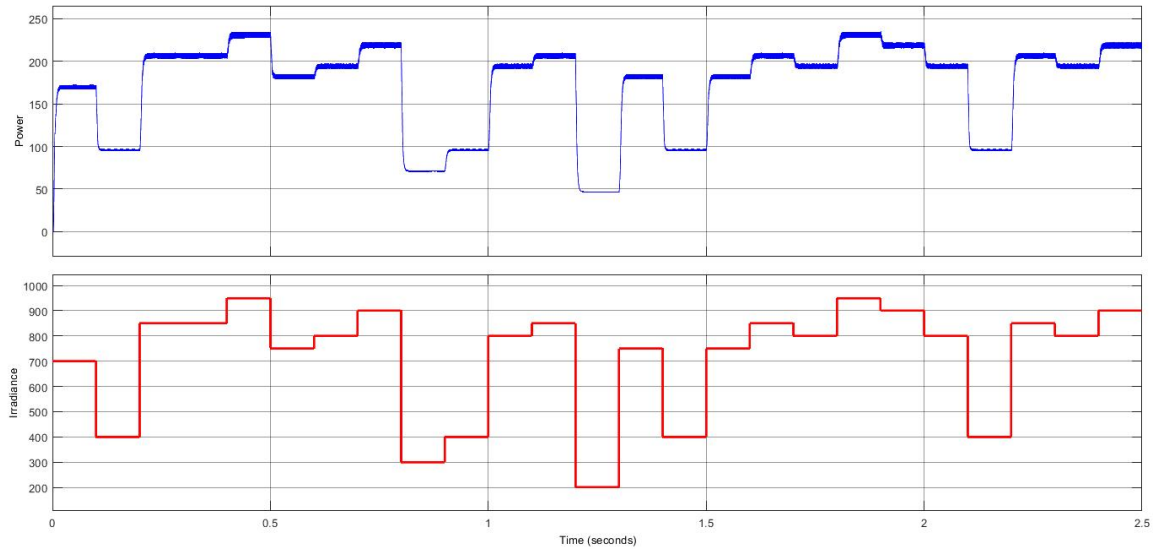

Figure 10. The occurrence of random fluctuations in amounts of incoming solar irradiance while concurrently maintaining a constant temperature of 25 C^o

Table 4. Performance metrics of the proposed algorithm under different irradiance conditions

No.	Time S	Irradiance (W/m^2)	Response time (S)	Ripple (%)	Efficiency (%)
1	0	700	0.002	1.73	98.8
2	0.1	400	0.1002	1.81	99.2
3	0.2	850	0.2003	1.78	98.8
4	0.3	850	0.3002	1.8	98.8
5	0.4	950	0.4002	1.78	98.8
6	0.5	750	0.5002	1.75	98.9
7	0.6	800	0.6002	1.7	98.8
8	0.7	900	0.7002	1.8	98.8
9	0.8	300	0.8002	1.75	99.2

No.	Time S	Irradiance *(W/m²)*	Response time (S)	Ripple (%)	Efficiency (%)
10	0.9	400	0.9003	1.78	99.1
11	1	800	1.002	1.7	98.5
12	1.1	850	1.1002	1.75	98.8
13	1.2	200	1.2002	1.73	99
14	1.3	750	1.3002	1.78	98.8
15	1.4	400	1.4002	1.8	99.1
16	1.5	750	1.5002	1.78	98.8
17	1.6	850	1.6002	1.75	98.8
18	1.7	800	1.7002	1.8	98.8
19	1.8	950	1.8002	1.75	98.8
20	1.9	900	1.9002	1.78	98.8
21	2	800	2.002	1.73	98.8
22	2.1	400	2.1002	1.7	99
23	2.2	850	2.2002	1.76	98.8
24	2.3	800	2.3002	1.78	98.8
25	2.4	900	2.4002	1.8	98.8

Under this approach, and to strengthen the statistical reliability of the proposed MPPT method, the results analyzed over multiple irradiance steps using mean and standard deviation metrics. The average ripple was 1.76 % with a very low standard deviation of 0.03 %, confirming stable tracking performance under variable irradiance. The average conversion efficiency remained high at 98.9 % with a standard deviation of 0.19 %. These small deviations indicate that the algorithm maintains consistent dynamic behavior despite rapid irradiance fluctuations. In addition, Friedman non-parametric test applied to the ripple, efficiency, and response-time measurements collected over irradiance transitions. Where each irradiance step treated as a block, while the three performance indicators considered as treatments. The test yielded a chi-square value of 50 and a p-value of $1.39\times10-11$, which is far below the 0.05 significance level. This result confirms that the observed variations among the three performance indicators are statistically significant; therefore, the proposed method exhibits a consistent and well-structured dynamic response to irradiance changes.

The real PV arrays introduce additional complexities such as partial shading, mismatch, and parasitic elements, which could alter the tracking dynamics. Thus, experimental testing is required to confirm the method's practical robustness.

CONCLUSION

PV systems are becoming increasingly popular as a reliable solution, aiming to reduce some of the complexities previously encountered and to incorporate solutions for tracking MPPT in variable solar radiation and fixed temperature. This involves a novel algorithm that adjusts the converter's duty cycle based on power output to track the MPP. The power output is the objective function, while the particles symbolize the potential duty cycles. The algorithm may struggle to adapt to dynamic irradiance changes; the proposed MPPT system seeks to improve tracking accuracy and speed through an enhanced VIPSO algorithm, demonstrating good PV system efficiency.

The novelty lies in the introduction of a dynamic initialization mechanism that triggers when the irradiance changes by more than 5%. This involves readjusting the particle positions and velocities to find the optimal solution, helping the algorithm adapt to the new conditions. Re-initialization guarantees that the algorithm effectively tracks the MPP during changes in irradiance by readjusting key parameters such as $Pbest$, $gbest$, and velocities.

To assess the robustness and statistical significance of the proposed VIPSO algorithm, each simulation scenario repeated 20 times with different random initializations of particle positions. The results averaged, and the corresponding standard deviations were calculated. The proposed algorithm introduces many contributions, including a current-sensitive reset strategy that maintains MPPT performance in real-time conditions, integration of dynamic behavior into the PSO framework without compromising convergence stability, and validation through simulations showing 99% efficiency, < 0.1s response time, and 1% ripple. The low output power ripple is its main strength, ensuring stable operation around the MPP even under rapidly changing irradiance and constant temperature. Statistical evaluation using the Friedman test further confirmed the consistency and robustness of the algorithm's dynamic response to changing environmental conditions, making VIPSO highly suitable for practical PV system applications.

REFERENCES

1. Zhang, L., et al., A modular grid-connected photovoltaic generation system based on DC bus. IEEE transactions on power electronics, 2010. 26(2): p. 523-531. https://doi.org/10.1109/TPEL.2010.2064337.
2. Liu, B., S. Duan, and T. Cai, Photovoltaic DC-building-module-based BIPV system—Concept and design considerations. IEEE Transactions on Power Electronics, 2010. 26(5): p. 1418-1429. https://doi.org/10.1109/TPEL.2010.2085087.
3. Sedaghati, Farzad, et al. "PV maximum power-point tracking by using artificial neural network." Mathematical Problems in Engineering 2012.1 (2012): 506709. https://doi.org/10.1155/2012/506709.
4. Feitosa, F., et al. (2025). "Evaluation of Photovoltaic Hydrogen Production Potential Along Highways Connecting the North and Northeast Regions of Brazil". Journal of Sustainable Development of Energy, Water and Environment Systems. Volume 13, Issue 2, June 2025, 1130574. http://dx.doi.org/10.13044/j.sdewes.d13.0574.
5. Iturralde Carrera, L.A., et al., Advances and Optimization Trends in Photovoltaic Systems: A Systematic Review. AI(MDPI), 2025. 6(9): p. 225. https://doi.org/10.3390/ai6090225.

6. Kumar, M., H.M. Niyaz, and R. Gupta, Challenges and opportunities towards the development of floating photovoltaic systems. Solar Energy Materials and Solar Cells, 2021. 233: p. 111408. https://doi.org/10.1016/j.solmat.2021.111408.
7. Adamu, Hassan, Francis Njoka, and Gideon Kidegho. "Performance of MPPT Charge Controller Under Moderate-to High-Temperature Field Condition." Journal of Sustainable Development of Energy, Water and Environment Systems 12.3 (2024): 1-15. http://dx.doi.org/10.13044/j.sdewes.d12.0504.
8. Sornek, Krzysztof, Wojciech Goryl, and Aleksandra Głowacka. "Improving the performance of photovoltaic panels using a direct water cooling system." Journal of Sustainable Development of Energy, Water and Environment Systems 11.4 (2023): 1-24. http://dx.doi.org/10.13044/j.sdewes.d11.0468.
9. Siddique, M. A. B., & Zhao, D. (2025). Emerging maximum power point control algorithms for PV systems: review, challenges and future trends. Electrical Engineering, 107, 9807–9839. https://doi.org/10.1007/s00202-025-03002-0.
10. Ali, M. H., et al. (2025). A comprehensive study of recent maximum power point tracking (MPPT) techniques for PV systems. Scientific Reports. https://doi.org/10.1038/s41598-025-96247-5.
11. Guo, S., et al., Efficient maximum power point tracking for a photovoltaic using hybrid shuffled frog-leaping and pattern search algorithm under changing environmental conditions. Journal of Cleaner Production, 2021. 297: p. 126573. https://doi.org/10.1016/j.jclepro.2021.126573.
12. Bugaje, Aminu, et al. "Investigating the performance of rural off-grid photovoltaic system with electric-mobility solutions: A case study based on Kenya." Journal of Sustainable Development of Energy, Water and Environment Systems 10.1 (2022): 1-15. https://doi.org/10.13044/j.sdewes.d9.0391.
13. Hida, Andi, et al. "Impact of Photovoltaic Penetration on the Distribution System Operation. Case Study Albania." Journal of Sustainable Development of Energy, Water and Environment Systems 13.2 (2025): 1-10. http://dx.doi.org/10.13044/j.sdewes.d13.0548.
14. Femia, N., et al., Optimization of perturb and observe maximum power point tracking method. IEEE transactions on power electronics, 2005. 20(4): p. 963-973. https://doi.org/10.1109/TPEL.2005.850975.
15. Yousaf, M.Z., et al., Improved MPPT of solar PV Systems under different Environmental conditions utilizes a Novel Hybrid PSO. Renewable Energy, 2025. 244: p. 122709. https://doi.org/10.1016/j.renene.2025.122709.
16. Yu, G.-R., Chang, Y.-D., & Lee, W.-S. (2024). Maximum Power Point Tracking of Photovoltaic Generation System Using Improved Quantum-Behavior Particle Swarm Optimization (IQPSO). Biomimetics, 9(4), 223. https://doi.org/10.3390/biomimetics9040223.
17. Renaudineau, H., et al., A PSO-based global MPPT technique for distributed PV power generation. IEEE Transactions on Industrial Electronics, 2014. 62(2): p. 1047-1058. https://doi.org/10.1109/TIE.2014.2336600.
18. Águila-León, J., et al. (2024). A meta-optimization approach with GWO-Enhanced PSO for MPPT in PV systems. Applied Energy. https://doi.org/10.1016/j.renene.2024.120892.
19. Arsad, A.Z., Zuhdi, A.W.M., Azhar, A.D., Chau, C.F., & Ghazali, A. (2025). Advancements in maximum power point tracking for solar charge controllers. Renewable and Sustainable Energy Reviews. https://doi.org/10.1016/j.rser.2024.115208.

20. Salah, C.B. and M. Ouali, Comparison of fuzzy logic and neural network in maximum power point tracker for PV systems. Electric Power Systems Research, 2011. 81(1): p. 43-50. https://doi.org/10.1016/j.epsr.2010.07.005.
21. Sedaghati, F., et al., PV maximum power-point tracking by using artificial neural network. Mathematical Problems in Engineering, 2012. 2012(1): p. 506709. https://doi.org/10.1155/2012/506709.
22. Badamchizadeh, M. and K. Madani. Applying modified discrete particle swarm optimization algorithm and genetic algorithm for system identification. in 2010 The 2nd International Conference on Computer and Automation Engineering (ICCAE). 2010. IEEE. https://doi.org/10.1109/ICCAE.2010.5451412.
23. Sundareswaran, K., et al., Enhanced energy output from a PV system under partial shaded conditions through artificial bee colony. IEEE transactions on sustainable energy, 2014. 6(1): p. 198-209. https://doi.org/10.1109/TSTE.2014.2363521.
24. Ibrahim, A., R. Aboelsaud, and S. Obukhov, Improved particle swarm optimization for global maximum power point tracking of partially shaded PV array. Electrical Engineering, 2019. 101: p. 443-455. https://doi.org/10.1007/s00202-019-00794-w.
25. Yoganandini, A. and G. Anitha, A modified particle swarm optimization algorithm to enhance MPPT in the PV array. International Journal of Electrical and Computer Engineering (IJECE), 2020. 10(5): p. 5001-5008. https://doi.org/10.11591/ijece.v10i5.
26. Zaghba, L., et al., An efficient, intelligent PSO-P&O-PI MPPT mechanism for Photovoltaic Systems under variable climatic conditions. Journal of Renewable Energies, 2024. 27(1): p. 15-33. https://doi.org/10.54966/jreen.v27i1.1137.
27. Mohammadinodoushan, M., et al., A new MPPT design using variable step size perturb and observe method for PV system under partially shaded conditions by modified shuffled frog leaping algorithm- SMC controller. Sustainable Energy Technologies and Assessments, 2021. 45: p. 101056. https://doi.org/10.1016/j.seta.2021.101056.
28. Li, Y., et al., Analysis and enhancement of PV efficiency with hybrid MSFLA–FLC MPPT method under different environmental conditions. Journal of Cleaner Production, 2020. 271: p. 122195. https://doi.org/10.1016/j.jclepro.2020.122195.
29. Anssari, et al., "Designing of a PSO-Based Adaptive SMC With a Multilevel Inverter for MPPT of PV Systems Under Rapidly Changing Weather Conditions". IEEE Access, 2024. 12: p. 41421-41435. https://doi.org/10.1109/ACCESS.2024.3377925.
30. Taha, M.Q., M.K. Mohammed, and B. El Haiba, Metaheuristic Optimization of Maximum Power Point Tracking in PV Array under Partial Shading. Engineering, Technology & Applied Science Research, 2024. 14(3): p. 14628-14633. https://doi.org/10.48084/etasr.7385.
31. Harrag, A. and S. Messalti, PSO-based SMC variable step size P&O MPPT controller for PV systems under fast changing atmospheric conditions. International Journal of Numerical Modelling: Electronic Networks, Devices and Fields, 2019. 32(5). https://doi.org/10.1002/jnm.2603.
32. Naidu, I.E.S., et al., A novel mine blast optimization algorithm (MBOA) based MPPT controlling for grid-PV systems. AIMS Electronics and Electrical Engineering, 2023. 7(2): p. 135-155. https://dx.doi.org/10.3934/electreng.2023008.
33. Syafii, et al. "Simple photovoltaic electric vehicles charging management system considering sun availability time." Journal of Sustainable Development of Energy, Water and Environment Systems 12.1 (2024): 1-12. https://doi.org/10.13044/j.sdewes.d11.0476.

34. Azzouzi, M., D. Popescu, and M. Bouchahdane, Modeling of Electrical Characteristics of Photovoltaic Cell Considering Single-Diode Model. Journal of Clean Energy Technologies, 2016. 4(6): p. 414-420. https://doi.org/10.18178/jocet.2016.4.6.323.
35. Ashraf, Nouman, et al. "Maximum Power Point Tracking Based Solar Powered Hybrid System of Constant Speed Induction Motor and Electrical Load under Partial Shading Condition using Priority Based Modelling." Journal of Sustainable Development of Energy, Water and Environment Systems, 2025, 1130622. https://doi.org/10.13044/j.sdewes.d13.0622.
36. Corcau, J.-I., L. Dinca, and E. Ureche, Comparative analysis of a dc to dc boost converter with constant and variable duty cycle, in 2015 9th International Symposium on Advanced Topics in Electrical Engineering (ATEE). 2015, IEEE. https://doi.org/10.1109/ATEE.2015.7133894.
37. Mohan, N., T.M. Undeland, and W.P. Robbins, "Power electronics: converters, applications, and design". 2nd edition, John wiley & sons INC. October 2002, 832 pages.
38. Byar, M., Chbirik, G., Brahmi, A., & Abounada, A. (2025). Hybrid ANN-PSO MPPT with high-gain boost converter for standalone photovoltaic systems. Electrical Engineering & Informatics. https://doi.org/10.11591/eei.v14i4.9451.
39. Mirjalili, S., et al., Particle swarm optimization: theory, literature review, and application in airfoil design. Nature-inspired optimizers: theories, literature reviews and applications, 2020: p. 167-184. https://doi.org/10.1007/978-3-030-12127-3_10.
40. Naser, A.T., et al., Performance Assessment of Meta-Heuristic MPPT Strategies for Solar Panels Under Complex Partial Shading Conditions and Load Variation. Global Energy Interconnection, 2025. Renewable Energy. https://doi.org/10.1016/j.gloei.2025.03.004.
41. Benuwa, B.B., et al., A comprehensive review of Particle swarm optimization. International Journal of Engineering Research in Africa, 2016. 23: p. 141-161. https://doi.org/10.4028/www.scientific.net/JERA.23.141.
42. Albright, L., and F. Vanek., "Energy Systems Engineering: Evaluation and Implementation". New York, NY, USA : McGraw-Hill, 2008.
43. Ngo, V.-Q.-B., et al., Improved krill herd algorithm based sliding mode MPPT controller for variable step size P&O method in PV system under simultaneous change of irradiance and temperature. Journal of the Franklin Institute, 2021. 358(7): p. 3491-3511. https://doi.org/10.1016/j.jfranklin.2021.02.021.
44. Manoharan, P., et al., Improved Perturb and Observation Maximum Power Point Tracking Technique for Solar Photovoltaic Power Generation Systems. IEEE Systems Journal, 2021. 15(2): p. 3024-3035. https://doi.org/10.1109/JSYST.2020.3003255.
45. Inomoto, R.S., J.R.B. de Almeida Monteiro, and A.J. Sguarezi Filho, Boost converter control of PV system using sliding mode control with integrative sliding surface. IEEE Journal of Emerging and Selected Topics in Power Electronics, 2022. 10(5): p. 5522-5530. https://doi.org/10.1109/JESTPE.2022.3158247.
46. Rahul, I. and R. Hariharan, Enhancement of solar PV panel efficiency using double integral sliding mode MPPT control. Tsinghua Science and Technology, 2023. 29(1): p. 271-283. https://doi.org/10.26599/TST.2023.9010030.
47. Singh, N., et al., A Flying Squirrel Search Optimization for MPPT Under Partial Shaded Photovoltaic System. IEEE Journal of Emerging and Selected Topics in Power Electronics, 2021. 9(4): p. 4963-4978. https://doi.org/10.1109/JESTPE.2020.3024719.

48. Djanssou, D.M., et al., Improvement of the Dynamic Response of Robust Sliding Mode MPPT Controller-Based PSO Algorithm for PV Systems under Fast-Changing Atmospheric Conditions. International Journal of Photoenergy, 2021. 2021: p. 1-13. https://doi.org/10.1155/2021/6671133.
49. Abdulridha, H.M., M. Shaker, and H.F. Jaafar, Tracking of Maximum Power Point for PV Solar System Based on Adaptive Quantum Neural Controller. International Journal of Intelligent Engineering & Systems, 2022. 15(3). https://doi.org/10.22266/ijies2022.0630.32.
50. Chellakhi, A., S. El Beid, and Y. Abouelmahjoub, An improved adaptable step-size P&O MPPT approach for standalone photovoltaic systems with battery station. Simulation Modelling Practice and Theory, 2022. 121: p. 102655. https://doi.org/10.1016/j.simpat.2022.102655.
51. Derrac, Joaquín, et al. "A practical tutorial on the use of nonparametric statistical tests as a methodology for comparing evolutionary and swarm intelligence algorithms." Swarm and Evolutionary Computation 1.1 (2011): 3-18. https://doi.org/10.1016/j.swevo.2011.02.002.

Paper submitted: 21.08.2025
Paper revised: 01.12.2025
Paper accepted: 16.12.2025